

Diffraction properties of two-dimensional photonic crystals

G. von Freymann^{a)}

Institut für Nanotechnologie, Forschungszentrum Karlsruhe in der Helmholtz-Gemeinschaft, 76021 Karlsruhe, Germany

W. Koch, D. C. Meisel, and M. Wegener

Institut für Angewandte Physik, Universität Karlsruhe (TH), 76128 Karlsruhe, Germany

M. Diem, A. Garcia-Martin, S. Pereira, and K. Busch

Institut für Theorie der Kondensierten Materie, Universität Karlsruhe (TH), 76128 Karlsruhe, Germany

J. Schilling, R. B. Wehrspohn, and U. Gösele

Max-Planck-Institut für Mikrostrukturphysik Halle, 06120 Halle, Germany

(Received 9 December 2002; accepted 28 May 2003)

We show that the envelope of the diffraction efficiency of a two-dimensional photonic crystal can exhibit spectral regions of very small diffraction efficiency ($< 5 \times 10^{-3}$), while in other regions, the diffraction efficiency is near unity. The experimental results on higher bands of hexagonal, silicon-based photonic crystals agree well with corresponding numerical calculations and highlight the prominent role of the surface termination, an aspect which cannot be described by the photonic band structure alone. We speculate about possible applications of such additional spectral filters in Raman and photoluminescence spectroscopy. © 2003 American Institute of Physics.

[DOI: 10.1063/1.1596731]

Photonic crystals (PCs)^{1,2} have recently attracted considerable attention because of their potential applications in telecommunication, as host for high finesse nanocavities, or as materials exhibiting negative refraction. Another interesting aspect, which was recently studied theoretically, is the use of two-dimensional PCs as diffraction gratings.^{3,4} As an electromagnetic plane wave hits the surface of a PC, the impedance mismatch between air and the PC leads to both, reflection and diffraction at the periodically modulated surface. A two-dimensional (2D) PC, illuminated perpendicular to the structure (see Fig. 1), diffracts within the plane of incidence—as a conventional surface diffraction grating—while three-dimensional (3D) PCs diffract off-plane as well.^{5,6} Thus, 3D-PCs are not considered in what follows. For a 2D-PC, the envelope of the diffraction efficiency in Littrow geometry, i.e., backscattering geometry, follows the usual formula³

$$m\lambda = 2s \sin \gamma,$$

with the surface lattice constant s , the diffraction order m , and the wavelength of light λ . The angle γ in the backscattering geometry is illustrated in Fig. 1. In a conventional surface diffraction grating—apart from some exceptions⁷—one usually has a smooth variation of the diffraction efficiency with incident wavelength with a maximum at the blaze angle. In contrast to this, it has recently been shown theoretically⁴ that a 2D-PC can exhibit spectral regions of very small diffraction efficiency—which we refer to as “3 holes” in the envelope of the diffraction efficiency. Apart from these holes, the diffraction efficiency of the 2D-PC can be close to 100%.

In this letter, we (i) give experimental evidence for the occurrence of such holes in Littrow geometry. (ii) Moreover, we show theoretically that the holes are *not* uniquely determined by the photonic crystal band structure alone, but are also determined by the *surface termination* of the photonic crystal. This allows for a detailed design of the 2D-PC diffraction properties, e.g., in order to selectively suppress certain frequencies such as the exciting laser line in Raman or in photoluminescence spectroscopy.

The samples investigated in our experiments are 2D-PCs with a hexagonal array of air holes (pores) of radius $r = 0.6 \mu\text{m}$ in silicon fabricated by electrochemical etching.⁸ The lattice constant is $a = 1.5 \mu\text{m}$. The height of the sample is about $100 \mu\text{m}$. One sample is “cut” along the ΓK direction (see Fig. 1), the other one along the ΓM direction. In the experimental setup, light from a halogen lamp is coupled into a balanced Michelson interferometer via a multimode optical fiber. At the end mirrors of this interferometer, one of which is replaced by the PC, the output of the multimode

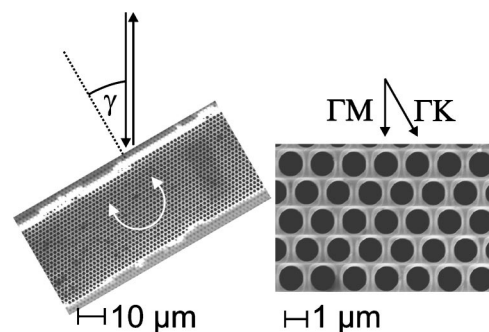


FIG. 1. One of the photonic crystals investigated, cut along the ΓK direction. The angle of incidence γ with respect to the normal coincide with the detection angle. The magnification shows the high quality of the internal structure. The ΓM and ΓK directions are emphasized.

^{a)}Electronic mail: georg.freymann@physik.uni-karlsruhe.de

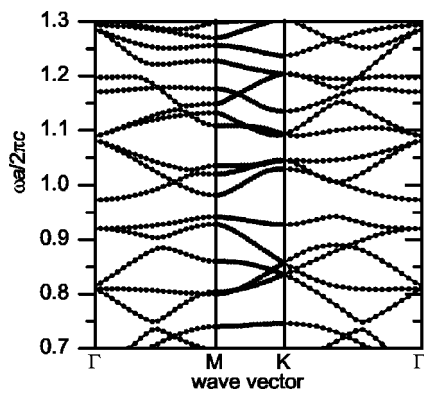


FIG. 2. Band structure of the higher-order bands for the photonic crystals investigated ($r/a=0.4$, H polarization). The fundamental band gap can be found around $\omega a/2\pi c_0=0.3$ and is not investigated in our experiments.

fiber is imaged to a spot diameter of about $100\ \mu\text{m}$, which illuminates the entire height of the sample. As usual, the spectrum is obtained from the Fourier transform of the interferogram. The photonic crystal is mounted on a rotational stage, which allows us to vary the angle of incidence—which equals the detection angle—with respect to the normal in the range from $\gamma=-5^\circ$ up to $\gamma=50^\circ$ in steps of $\Delta\gamma=24\ \text{min}$. All experiments are performed for the H polarization, which means that the electric field vector is perpendicular to the pores. Diffraction occurs only for sufficiently high frequencies with $\omega a/2\pi c_0 \geq 1/2$ in case of propagation along the ΓM direction or for $\omega a/2\pi c_0 \geq 1/(2\sqrt{3})$ in case of propagation in the ΓK direction.³ (These frequencies would be lowered by a factor of $1/n_{\text{med}}$, if the photonic crystal is embedded in a material with a higher index of refraction n_{med} than air).⁹ The fundamental band gap of these PBG structures is centered around $\omega a/2\pi c_0=0.3$. Thus, we perform the experiments on higher bands in the bandstructure (see Fig. 2). It is clear that the higher bands are more sensitive to any type of disorder or imperfections, which has so far hindered detailed experimental investigations. In turn, the occurrence of well-defined diffraction peaks can be taken as an indication of high sample quality.

Figure 3(a) shows the experimental result for the sample cut along the ΓK direction. The intensity diffraction efficiency spectra (logarithmic scale) are plotted between $\omega a/2\pi c_0=0.7$ and $\omega a/2\pi c_0=1.3$ over the angle of incidence γ . At $\gamma=0^\circ$ the usual reflection spectrum under perpendicular incidence is detected. As expected it is modulated with the optical properties of the photonic crystal: Complete band gaps, stop gaps for certain directions, flat and symmetry forbidden bands lead to high reflectivity (compare with Fig. 2). For increasing angle, the intensity sharply decreases and finally vanishes until the first surface Bragg order appears at $\gamma \approx 23^\circ$ for $\omega a/2\pi c_0=1.3$. Its envelope follows that of a simple surface diffraction grating. In addition, the first Bragg order is modulated due to the 2D-PC. The light enters the photonic crystal, couples to Bloch modes and propagates into the sample. Therefore, frequencies with high coupling efficiencies are not diffracted into backward direction. The arrow in Fig. 3(a) marks a position with diffraction efficiency below 5×10^{-3} . Figure 3(b) shows cuts at different spectral positions ($\omega a/2\pi c_0=0.85, 1.0, 1.15$), which are indicated by the dashed lines in Fig. 3(a). For $\omega a/2\pi c_0=0.85$ no diffrac-

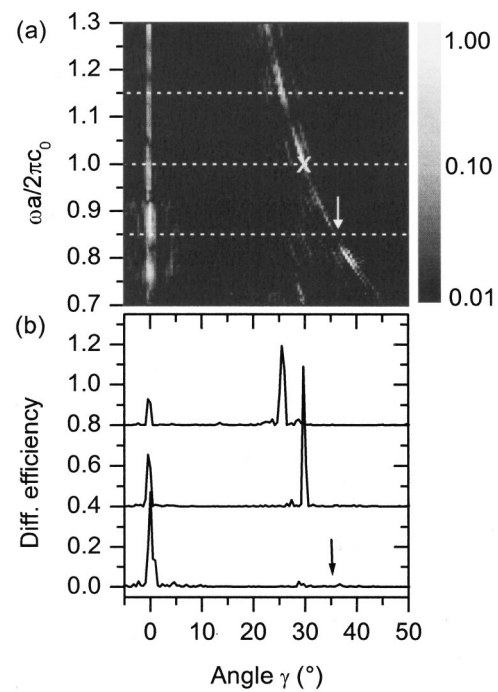


FIG. 3. (a) Measured intensity diffraction efficiency for a cut along the ΓK direction. The arrow marks a region of diffraction efficiency $< 5 \times 10^{-3}$. The cross marks the position of the Bragg reflex expected for an ideal 2D structure. (b) Cuts at selected spectral positions, as marked by the dotted lines in (a). The spectra are vertically offset for clarity.

tion peak is observed. Note that a very simple calculation for an ideal hexagonal structure along the lines of Bragg-diffraction predicts only one isolated Bragg reflex at the position marked by the cross in Fig. 3(a)—and no continuous envelope. The same behavior is observed for the sample cut along the ΓM direction (not shown). Apart from the theoretically predicted Bragg orders, additional “speckle-like” stripes can be observed in Fig. 3. They seem to be directly related to surface disorder—for instance missing or incompletely cut pores (see Fig. 1)—because they are also observable in results obtained from surface diffraction gratings (not shown).

At first sight it is not clear, which frequencies will be diffracted under certain angles and which will not. The reflection spectrum at zero degrees corresponds to spectroscopy along the ΓM (ΓK) direction. For instance rotating the sample about 30° means changing the direction of spectroscopy from ΓM to nearly ΓK and vice versa (here the refraction at the surface has to be accounted for). This hinders a direct comparison with bandstructure calculations as shown in Fig. 2. In order to compare the measurements with calculations, we have computed the reflection properties of the samples following the scattering-matrix approach by Whittaker and Culshaw.¹⁰ A scattering-matrix approach allows accurate calculations of the reflection and transmission properties of deeply patterned diffraction gratings as well as photonic crystal slabs. In this calculation, we consider the Poynting vector for Bragg orders, which are backscattered into a cone with an opening angle of 1.5° around the incoming direction. We include slight absorption ($n=3.45+i0.015$) in the calculations to suppress Fabry-Pérot-modes, which are not observed in the experiment either. In addition, we perform the calculations for different surface

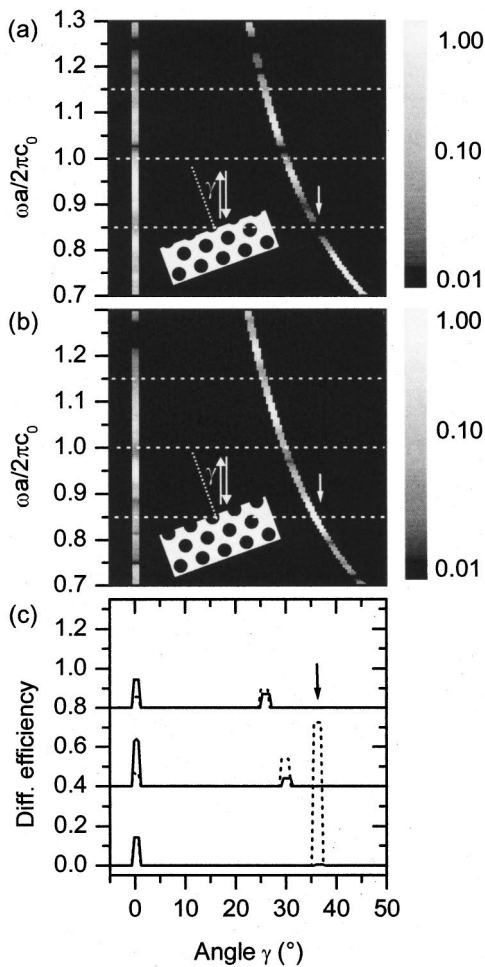


FIG. 4. (a) Complete numerical simulation for a 2D-PC cut along the ΓM direction. (b) Same as (a) but for a different surface termination as indicated by the insets. The arrows mark the same position as in the experiment [see Fig. 3(a)]. (c) Cuts at the same positions as in the experiment. The solid curves correspond to (a), the dotted ones to (b).

terminations, indicated by the insets in Fig. 4. The results of the complete numerical calculations are shown in Figs. 4(a) and 4(b). The angular behavior is well reproduced. As in the experiment the diffraction efficiency is quite low for certain frequencies [see arrow in Fig. 4(c)]. The calculated diffraction efficiency at this point is $<4 \times 10^{-3}$ and with this comparable to the experimental result (there $<5 \times 10^{-3}$). Furthermore, the spectral behavior is strongly influenced by the surface termination of the photonic crystal—a fact well known, e.g., from dielectric mirrors, but not emphasized so far for photonic crystals: The diffraction efficiency changes for instance from near zero in Fig. 4(a) to near unity in Fig. 4(b) at the position marked by the arrow [Fig. 4(c)]. Similarly, the reflection spectrum under perpendicular incidence is strongly influenced too. We interpret this behavior as an

interference effect between the light diffracted by the surface corrugation and the light scattered from the Bloch modes of the bulk photonic crystal. Or spoken in terms of a simple analogy, the surface termination acts like a very special antireflection coating. Due to the somewhat undefined surface termination in the experiment (see Fig. 1), we do not expect perfect agreement between experiment and theory. Nevertheless, we find a good qualitative agreement, especially for the suppressed diffraction efficiency at the position of the arrows. Therefore, a well designed photonic crystal with a disorder free and well terminated surface in a single pass spectrometer will efficiently suppress intense narrow laser lines. For this purpose the photonic crystal is designed in such a way that the laser frequency is placed in the discussed hole of low diffraction efficiency. This would allow the undisturbed detection of weak Raman or photoluminescence lines which are spectrally nearby but already out of the hole of low diffraction efficiency.

In conclusion, we have presented angle and spectrally resolved Bragg-diffraction measurements on 2D photonic crystals. We have shown that they exhibit an angular behavior similar to that of ordinary surface diffraction gratings but modulated with the optical properties of the photonic crystal. In addition complete numerical calculations show good qualitative agreement with the experimental results and illustrate the crucial influence of the surface termination. For certain frequencies we find diffraction efficiencies below 5×10^{-3} . The observed effects might be useful for Raman or photoluminescence spectroscopy.

The authors acknowledge support by the Deutsche Forschungsgemeinschaft (DFG) through the DFG-Forschungszentrum “Functional Nanostructures” (DFG-CFN). The research of A.G.-M. and K.B. is further supported by DFG-Project No. Bu 1107/2-2 (Emmy-Noether program), that of M.W. by the DFG Leibniz-award 2000. The authors thank A. Birner and F. Müller for the initial preparation of the samples.

¹E. Yablonovitch, Phys. Rev. Lett. **58**, 2059 (1987).

²S. John, Phys. Rev. Lett. **58**, 2486 (1987).

³D. Maystre, Opt. Express **8**, 209 (2001).

⁴M. Doosje, B. J. Hoenders, and J. Knoester, Opt. Commun. **206**, 253 (2002).

⁵H. M. van Driel and W. L. Vos, Phys. Rev. B **62**, 9872 (2000).

⁶S. G. Romanov, T. Maka, C. M. Sotomayor Torres, M. Müller, R. Zentel, D. Cassagne, J. Manzanares-Martinez, and C. Jouanin, Phys. Rev. E **63**, 056603 (2001).

⁷R. Petit, *Electromagnetic Theory of Gratings* (Springer, Berlin, 1980).

⁸A. Birner, R. B. Wehrspohn, U. M. Gösele, and K. Busch, Adv. Mater. (Weinheim, Ger.) **13**, 377 (2001).

⁹D. Labilloy, H. Benisty, C. Weisbuch, T. F. Krauss, R. M. De La Rue, V. Bardinal, R. Houdr, U. Oesterle, D. Cassagne, and C. Jouanin, Phys. Rev. Lett. **79**, 4147 (1997).

¹⁰D. M. Whittaker and I. S. Culshaw, Phys. Rev. B **60**, 2610 (1999).